

Convection-driven grooved terrain formation on Ganymede: Predictions for JUICE

N. P. Hammond and A. C. Barr

Brown University, Providence, RI, 02912, USA (noah_hammond@brown.edu)

Abstract

Grooved terrain covers over half of the surface of Ganymede, Jupiter's largest ice/rock moon and target for the forthcoming JUICE mission. Mechanisms proposed for the formation of grooved terrain include extensional faulting, cryovolcanism and convection-driven lithospheric spreading. Here, we show that convecting ice shells 10 to 80 km thick with surface viscosities of $\sim 10^{17.5}$ Pa s can create both the heat flux and the strain rate inferred for the formation of grooved terrain. We find that surface conditions above convective downwellings are consistent with the heat flux inferred for dark terrain and conditions favorable for the formation of long wavelength compressional folds. Therefore, high resolution topographic mapping from JUICE may reveal long wavelength folds perpendicular to and 10 to 80 km from the boundaries of linear groove lanes.

1. Introduction

The surface of Ganymede is divided into heavily cratered dark terrain and the relatively young, light grooved terrain [1]. Grooves consist of sub-parallel ridges and troughs [2] spaced ~ 7 km apart, which are often subdivided by narrower grooves 100 m – 1 km wide [1]. A subset of groove lanes, called subdued grooves, are smoother and brighter in appearance and show no obvious lineations at the ~ 1 km scale [3]. Grooves are interpreted as extensional features that formed during an era of global expansion, which may have resulted from satellite differentiation [4] or melting of the ice I shell when Ganymede entered a possible Laplace-like resonance with neighboring satellites [5]. Tensional stresses in the lithosphere may then cause grooves to form by tilt-block style normal faulting or horst and graben formation [2].

Convection in Ganymede's ice shell has been suggested as a possible driving mechanism for grooved terrain formation [6]. Head et al., [7] argued that subdued groove lanes on Ganymede form by a similar mechanism to extensional bands on Europa, which may form by convection-driven lithospheric spreading [8]. However, previous work suggested

that convective stresses are not strong enough to drive surface deformation on Ganymede [9], and that convection would remain confined below a "stagnant lid", a cold and highly viscous layer of ice which limits heat transport and inhibits resurfacing. However, if the near-surface ice has a yield stress comparable to or lower than the thermal buoyancy stresses from convection, plumes can reach close to the surface to drive deformation [10, 11].

This style of "sluggish lid" convection may be occurring at the active Enceladus South Polar terrain (SPT) [11]. Barr [11] showed that the heat flows and strain rates associated with sluggish lid convection are consistent with the observed heat flow and surface age of the Enceladus SPT. For grooved terrain on Ganymede, the heat flux estimated from flexure, $F > 100$ mW m⁻² [12], and strain rates estimated from extensional necking models, $10^{-13} - 10^{-16}$ s⁻¹ [13], resemble the heat flux and strain rate of the Enceladus SPT. The similarity between the heat flow and deformation rates for grooved terrain and the SPT, and possible evidence for lithospheric spreading along subdued grooves [7], suggest that grooved terrain may have formed by convection driven resurfacing. Here, we test this hypothesis using models of solid-state convection in Ganymede's ice shell.

2. Methods

We use the finite element model CITCOM [14] to model convection for a wide range in ice shell conditions. We vary the Rayleigh number, which controls the vigor of convection and is related to the ice shell thickness D by,

$$Ra = \rho g \alpha \Delta T D^3 / (\kappa \eta), \quad (1)$$

where $\rho = 1000$ kg m⁻³, is the density of ice, $g=1.43$ m s⁻² is the surface gravity on Ganymede, $\alpha=10^{-4}$ K⁻¹ is the coefficient of thermal expansion, η is the viscosity of ice, $\kappa=10^{-6}$ m² s⁻¹ is the thermal diffusivity, and $\Delta T = 150$ K is the temperature

contrast between the surface and the base of the ice shell. Viscosity varies as a function of temperature as,

$$\eta(T) = \eta_0 \exp(-\theta T / \Delta T), \quad (2)$$

where $\eta_0 = \eta_1 \Delta \eta$, $\eta_1 = 10^{14}$ Pa s is the melting point viscosity (eg., [15]), $\theta = \ln(\Delta \eta)$, and $\Delta \eta$ is the viscosity contrast between ice at the surface and ice near the melting point.

We vary $\Delta \eta$ between $10^{3.25}$ Pa s and 10^4 Pa s to mimic the effect of an upper surface whose yield stress is less than the critical stress for sluggish lid convection due to impact fracturing, tidal flexing, and/or shallow tidal heating (cf., [16, 17]). We vary the basal Rayleigh number between $10^{5.5}$ and 10^8 . We assume a basally heated shell and neglect tidal heating, because the strong dependence of viscosity on temperature is the key control on the heat flow and near-surface behavior [16].

We allow our simulations to reach steady-state solutions and then measure how heat flux and strain rate vary at the surface. Successful simulations have regions with a heat flux > 100 mW m $^{-2}$ and a strain rate between 10^{-16} and 10^{-13} s $^{-1}$.

3. Results

For a melting point viscosity of 10^{14} Pa s, we find that ice shells 10 to 80 km thick with surface viscosities of $\sim 10^{17.5}$ Pa s are conducive to forming grooved terrain. Figure 1 shows an example result where regions above convective upwellings are consistent with grooved terrain conditions, ($F \sim 100$ mW m $^{-2}$ and $\dot{\epsilon} = 10^{-13}$ to 10^{-14} s $^{-1}$), and conditions in the regions of compression are consistent with the maximum heat flux estimated for dark terrain [18].

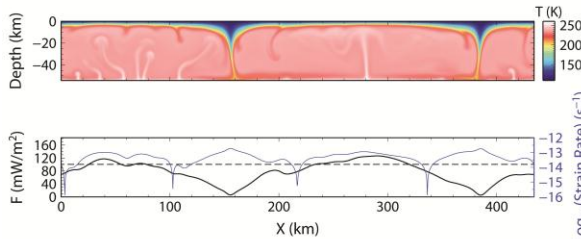


Figure 1: (top) Temperature field for a convecting ice shell on Ganymede that is 54 km thick, with $Ra_1=10^{7.5}$, $\Delta \eta=10^{3.75}$. (bottom) Heat flux (black) and strain rate (blue) as a function of horizontal distance. Groove lanes are inferred to form between $x=20$ to 60 and 250 to 320 km; compressional regions where we predict folding occur between $x=100$ to 200 and 350 to 450 km.

Galileo observations suggest that the total surface strain recorded on Ganymede may be larger than the

~3% possible from differentiation [19]. If grooved terrain formed by convection-driven resurfacing, surface strain would likely exceed the strain expected from global expansion and compressional features would form at the surface. However, compressional features have not yet been observed on Ganymede.

On Europa, long-wavelength folds, identified by Prockter and Pappalardo [20] are suggested to balance the strain from extensional bands. Bland and McKinnon [21] show that fold formation and lithospheric thickening on Europa can occur for strain rates of 10^{-12} to 10^{-15} s $^{-1}$ and $F = 20$ to 100 mW m $^{-2}$, similar to the conditions we find above convective downwelling regions, implying that fold formation may have occurred on Ganymede.

If convection is the driving force for grooved terrain formation, high resolution mapping from ESA's upcoming JUICE mission may be able to identify the long-wavelength folds that should balance the extension driven by convection. Detection of long wavelength folds and stratigraphic evidence for pervasive lithospheric spreading along subdued grooves would represent strong evidence for convective stresses having played a prominent role in the formation of grooved terrain.

Acknowledgements: This work is supported by NASA PG&G grant NNX12AI76G.

4. References

- [1] Collins G., et al., (1998) *GRL* 25, 3, 233–236. [2] Pappalardo R., et al., (1998) *Icarus* 135, 276-302. [3] Patterson W. et al., (2010) *Icarus* 207, 2, 845-867. [4] Squyres S., (1980) *GRL* 7, 593-59. [5] Bland T. & Showman A. (2007), *Icarus* 189, 439–456. [6] Lucchitta B., (1980) *Icarus* 44, 481-501. [7] Head J., et al., (2002) *GRL* 29, 2151. [8] Prockter L., et al., (2002) *JGR* 107, E5 5028. [9] Squyres W. & Croft K. (1986) *Satellites*, p. 293 – 341. [10] Showman A. & Han L. (2005) *Icarus*, Volume 177, Issue 2, p. 425-437. [11] Barr A. C. (2008) *JGR* 113, E07009 14. [12] Nimmo F., et al. (2002) *GRL* 29, 62-65. [13] Bland M. & Showman A. (2007), *Icarus* 189, 439–456. [14] Moresi, L. & Solomatov V., (1995) *Phys. Fluids*, 7, 2154-2162. [15] Barr A. & McKinnon W., (2007) *JGR* 112, E2, E02012. [16] Solomatov, V., (2004) *JGR* 109, B01412. [17] Roberts J. & Nimmo F., (2008) *GRL* 25, 9, L09201 [18] Nimmo F. & Pappalardo R. (2004) *GRL* 31, L19701 [19] Collins G. C. (2008) *LPSC XXXIX*, 2254. [20] Prockter L. & Pappalardo R. (2000) *Science*, 289, 5481, 941-944. [21] Bland M. & McKinnon W. (2012) *Icarus*, 221, 2, 694-709